University of Wollongong
Research Online

Australian Institute for Innovative Materials - Papers

Australian Institute for Innovative Materials

2014

Electrochemical nonenzymatic sensor based on CoO decorated reduced graphene oxide for the simultaneous determination of carbofuran and carbaryl in fruits and vegetables

MingYan Wang
University of Wollongong, mingyan@uow.edu.au

JunRao Huang
HuaiHai Institute of Technology

Meng Wang
University of Wollongong, mw088@uowmail.edu.au

DongEn Zhang
Huaihai Institute of Technology

Jun Chen
University of Wollongong, junc@uow.edu.au

Follow this and additional works at: https://ro.uow.edu.au/aiimpapers

 Part of the Engineering Commons, and the Physical Sciences and Mathematics Commons

Research Online is the open access institutional repository for the University of Wollongong. For further information contact the UOW Library: research-pubs@uow.edu.au

Electrochemical nonenzymatic sensor based on CoO decorated reduced graphene oxide for the simultaneous determination of carbofuran and carbaryl in fruits and vegetables

Abstract

A novel nonenzymatic sensor based on cobalt (II) oxide (CoO)-decorated reduced graphene oxide (rGO) was developed for the detection of carbofuran (CBF) and carbaryl (CBR). Two well-defined and separate differential pulse voltammetric peaks for CBF and CBR were obtained with the CoO/rGO sensor in a mixed solution, making the simultaneous detection of both carbamate pesticides possible. The nonenzymatic sensor demonstrated a linear relationship over a wide concentration range of 0.2–70 μM (R = 0.9996) for CBF and 0.5–200 μM (R = 0.9995) for CBR. The lower detection limit of the sensor was 4.2 μg/L for CBF and 7.5 μg/L for CBR (S/N = 3). The developed sensor was used to detect CBF and CBR in fruit and vegetable samples and yielded satisfactory results.

Keywords

oxide, simultaneous, determination, carbofuran, fruits, carbaryl, vegetables, electrochemical, nonenzymatic, sensor, coo, decorated, reduced, graphene

Disciplines

Engineering | Physical Sciences and Mathematics

Publication Details

Wang, M., Huang, J., Wang, M., Zhang, D. & Chen, J. (2014). Electrochemical nonenzymatic sensor based on CoO decorated reduced graphene oxide for the simultaneous determination of carbofuran and carbaryl in fruits and vegetables. Food Chemistry, 151 191-197.

This journal article is available at Research Online: https://ro.uow.edu.au/aiimpapers/973

Electrochemical nonenzymatic sensor based on CoO decorated reduced graphene oxide for the simultaneous determination of carbofuran and carbaryl in fruits and vegetables

MingYan Wang [a,b,⇑], JunRao Huang [a], Meng Wang [b], DongEn Zhang [a], Jun Chen [b,⇑]

[a] Department of Chemical Engineering, Huaihai Institute of Technology, Lianyungang 222005, China
[b] Intelligent Polymer Research Institute, ARC Centre of Excellence for Electromaterials Science, Australian Institute of Innovative Materials, University of Wollongong, Northfields Avenue, Wollongong, NSW 2522, Australia

a r t i c l e i n f o

Article history:
Received 5 August 2013
Received in revised form 7 October 2013
Accepted 10 November 2013
Available online 18 November 2013

Keywords:
Carbamate pesticides
Cobalt (II) oxide
Reduced graphene oxide
Nonenzymatic
Sensor

a b s t r a c t

A novel nonenzymatic sensor based on cobalt (II) oxide (CoO)-decorated reduced graphene oxide (rGO) was developed for the detection of carbofuran (CBF) and carbaryl (CBR). Two well-defined and separate differential pulse voltammetric peaks for CBF and CBR were obtained with the CoO/rGO sensor in a mixed solution, making the simultaneous detection of both carbamate pesticides possible. The nonenzymatic sensor demonstrated a linear relationship over a wide concentration range of 0.2–70 **l**M (R = 0.9996) for CBF and 0.5–200 **l**M (R = 0.9995) for CBR. The lower detection limit of the sensor was 4.2 **l**g/L for CBF and 7.5 **l**g/L for CBR (S/N = 3). The developed sensor was used to detect CBF and CBR in fruit and vegetable samples and yielded satisfactory results.

2013 Elsevier Ltd. All rights reserved.

1. Introduction

Carbamate compounds are the most widely used pesticides in agriculture because of their high insecticidal activity (Garbellini, Salazar-Banda, & Avaca, 2009; Nikolelis, Raftopoulou, Psaroudakis, & Nikoleli, 2008). However, carbamate pesticides used indiscriminately can bioaccumulate in food and water sources with subsequent bioconcentration through the food chain (Moraes, Mascaro, Machado, & Brett, 2009). These organic toxins enter human bodies through the food chain or drinking water and threaten human health with their toxicity to acetylcholinesterase (AChE), an en- zyme essential for the function of the central nervous system in humans (Firdoz et al., 2010). Thus, sensitive, accurate, and rapid detection of these carbamate pesticides is important to protect the environment and human health.

Detection of carbamate pesticides was generally carried out by gas chromatography (Cavaliere, Monteleone, Naccarato, Sindona, & Tagarelli, 2012), high performance liquid chromatography (HPLC) (Song, Shi, & Chen, 2013), flow-injection chemiluminescence (Sanchez-Barragan, Karim, Costa-Fernadez, Piletsky, & Sanz-Medel, 2007), fluorimetry (Veglia, 2000) and competitive immunoassays and immunosensors (March, Manclus, Jimenez, Arnau, & Montoya, 2009; Sun, Du, & Wang, 2012). However, some of these techniques are time consuming and often require expensive instrumentation and toxic organic reagents, making them complicated and thus unsuitable for field routine operation. In recent years, electrochemical techniques have drawn the interest of researchers because of their advantages, such as low cost, easy operation, fast response, and high sensitivity (Du et al., 2008; Oliveira et al., 2013). Numerous enzyme-based biosensors have been developed for the detection of carbamate pesticides based on their inhibition of the enzymatic reaction of AChE (Cesarino, Moraes, Lanza, & Machado, 2012; Liu et al., 2011). However, enzymes used as medium for sensors always need special care in terms of temperature, pH, applied potential, storage, and enzyme activity, making these systems more difficult to work with and less robust. Considerable attention has been focused on the development of novel nonenzymatic electrodes to avoid the disadvantages of enzyme-based sensors. Transition metal compounds have received significant attention because of their high catalytic activity, low cost, and environment friendliness. Moraes et al. (2009) reported the utilisation of multiwall carbon nanotubes with cobalt phthalocyanine for the direct quantitative determination of carbaryl in natural waters. A self-assembled monolayer film of tetra-substituted cobalt, iron, and

⇑ Corresponding authors. Addresses: Department of Chemical Engineering, Huaihai Institute of Technology, Lianyungang 222005, China. Tel.: +86 518 85895409; fax: +86 518 85895401 (M. Wang), Intelligent Polymer Research Institute, ARC Centre of Excellence for Electromaterials Science, Australian Institute of Innovative Materials, University of Wollongong, Northfields Avenue, Wollongong, NSW 2522, Australia . Tel.: +61 2 42213781; fax: +61 2 42213114 (J. Chen).
E-mail addresses: mingyanlyg@hotmail.com (M. Wang), junc@uow.edu.au (J. Chen).

manganese alkylthio phthalocyanine compounds on a gold electrode was successfully applied for the direct detection of carbofuran (Akinbulu, Khene, & Nyokong, 2010). However, only a few studies regarding the immobilization of transition metal oxides for the electrocatalytic oxidation of carbamate pesticides have been reported. The application of transition metal oxides as catalysts is limited by their relatively poor electrical conductivity and low electron transfer rate. Recently, reduced graphene oxide (rGO) has received significant attention as an ideal support material for transition metal oxides because of its large surface area and high electrical conductivity. The integration of graphene and metal nanoparticles elicits synergistic effects in electrocatalytic application (Zhang, Long, Zhang, Du, & Lin, 2012). Thus, the integration of rGO and cobalt (II) oxide may have a similar effect on the electrocatalytic oxidation of carbamate pesticides.

In the present work, a novel electrochemical sensor based on CoO nanoparticle-decorated rGO modified glassy carbon electrode (GCE) was fabricated. The as-prepared CoO/rGO sensor exhibited a significant enhancement in electrocatalytic performance for carbofuran (CBF) and carbaryl (CBR) oxidation. A very good resolution of voltammetric peaks of these two carbamate pesticides in the mixed solution was obtained by this novel sensor, and a differential pulse voltammetric (DPV) technique was developed for the simultaneous detection of CBF and CBR in the mixture. CoO/rGO/GCE exhibited a relatively high sensitivity as an amperometric sensor and was employed for the first time for the simultaneous detection of CBF and CBR in fruit and vegetable samples.

2. Experimental

2.1. Reagents and apparatus

A 1.0×10^{-2} mol/L stock solution of each pesticide, carbofuran (99.8% purity, Sigma–Aldrich, Germany) and carbaryl (99.8% purity, Sigma–Aldrich, Germany), isoprocarb (99.5% purity, Aladdin, China), methiocarb (99.8% purity, Aladdin, China), and propoxur (99.5% purity, Aladdin, China) were prepared daily in acetonitrile (Chromatographic, Sigma–Aldrich, Germany). The direct electrochemical detection of carbamate residues without the need for previous hydrolysis of the target analysts has been reported (Codognoto et al., 2006; Moraes et al., 2009; Rao, Loo, Sarada, Terashima, & Fujishima, 2002). The relatively high potential required for the detection of these pesticides strongly affects the detection limits and selectivity. According to earlier research, the hydrolysed derivatives of the carbamate by alkaline solution exhibited a much lower oxidation potential and good electrochemical response, minimising the interference and dramatically increasing the electrode sensitivity (Akinbulu et al., 2010; Akinbulu, Ozoemena, & Nyokong, 2011; Wei, Sun, Wang, Li, & Chen, 2008). Thus, electrochemical analysis of carbofuran, carbaryl, isoprocarb, methiocarb and propoxur was preceded by hydrolysis of a given volume of the stock solution in a 0.5 mol/L NaOH solution for 10 min at 50 °C. Aliquot of the hydrolyzate were diluted in a suitable electrolyte for the voltammetric experiments. All chemicals were analytical reagent grade and used without further purification. All solutions were prepared with ultrapure water of resistivity 18.2 MΩ cm obtained from a Millipore Milli-Q system.

Electrochemical measurements were performed using a CHI 660B electrochemical workstation (Austin, USA) with a conventional three-electrode cell. A bare or modified glassy carbon electrode (GCE) was used as working electrode. A platinum wire was used as the counter electrode and a 3 M KCl saturated Ag/AgCl electrode as the reference electrode, respectively.

The crystalline properties and morphologies of the as-prepared materials were characterised by powder X-ray diffraction (XRD, D8-advanced, Bruker, 40 kV, 20 mA, Cu Ka radiation) and scanning electron microscopy (SEM, JEOL, JSM6700F) equipped with an X-ray energy dispersive spectrometer (EDS). The atomic composition of the samples was detected by X-ray photoelectron spectroscopy (XPS, Perkin Elmer, Al Ka radiation). HPLC detection was carried out with an Agilent 1100 coupled with a UV–Vis detector, and the column was C18 analytical column (4.6 mm × 150 mm, 5 μm).

2.2. Synthesis of CoO/rGO nanocomposite

Graphene oxide (GO) was synthesized by the modified Hummers method (Hummers & Offeman, 1958). The CoO/rGO nanocomposite was synthesized as the following procedures. Firstly, 2 mmol $Co(Ac)_2\ 4H_2O$ and 2 mmol $CO(NH_2)_2$ were dissolved into 30 mL distilled water. Then, GO powders (with various mass weights) were added into the above solution and sonicated for 1 h, followed with an addition of 1 mL hydrazine hydrate and magnetically stirred for 6 h at room temperature. The as-prepared solution was then transferred into a Teflon liner, which was sealed in a steel autoclave. The autoclave was maintained at 190 °C for 2 h and then was allowed to cool down to room temperature by a cool-water system. The resulting precipitate was separated by filtration, and washed with ultrapure water and absolute ethanol for 5 times and then dried in vacuum at 60 °C. Finally, the black-colour CoO/rGO powder was obtained via heating the precipitate to 500 °C for 5 h at a heating rate of 5 °C/min under nitrogen atmosphere. For comparison pure CoO powder without rGO and rGO without CoO were also prepared under identical conditions.

2.3. Preparation of CoO/rGO modified GCE (CoO/rGO/GCE)

The GCE was polished to a mirror-like surface with 1.0, 0.3 and 0.05 μm alumina slurry followed by rinsing thoroughly with ultrapure water and dried with fluid stream of highly purified nitrogen before use. For preparation of the working electrodes, required amount of the CoO/rGO nanocomposites ultrasonically dispersed in 0.081% Nafion solution to obtain a 2 mg/mL uniform ink. Then 10 μL of the ink was dropped on the GCE and dried in the air before the electrochemical tests. The catalyst loading on the electrode was maintained as 80 $\mu g\ cm^{-2}$ for all the electrochemical testing. For comparison CoO or rGO modified GCE were also prepared under equal processes.

2.4. Electrochemical measurement

Cyclic and differential pulse voltammetry measurements were carried out in unstirred electrolyte at room temperature. All potentials were measured and reported vs. Ag/AgCl. In a typical process, 100 mL electrolyte was transfer into a clean electrochemistry cell, and then the required volume of samples was added by micropipette. After accumulation for 300 s at open circuit potential, cyclic voltammetry (CV) was performed from −0.2 to 1.0 V with the scan rate of 100 mV/s. The differential pulse voltammetry (DPV) was carried out from 0.1 to 1.0 V with the following parameters: amplitude, 0.05 V; pulse width, 0.05 s; sample width, 0.05 s; pulse period, 0.2 s; quiet time, 2 s.

2.5. Sample preparation

The grapes, oranges, tomatoes and cabbages (from local market) were cut into small pieces, respectively. The fruit and vegetable samples (10 g) were exactly weighed and 50 mL electrolyte was added. The mixtures were put into a stainless steel blender to be homogenised. The pulp samples were shaken vigorously by ultrasonication for 60 min. Then the samples were centrifuged and the supernatant were collected and diluted. The analysis of

carbofuran and carbaryl were performed using the standard addition method. The results were obtained from an average of three parallel experiments.

2.6. HPLC measurements

The HPLC measurements were performed in triplicate. For determination of carbofuran and carbaryl, the mobile phase consisted of a mixture of acetonitrile and water 65:35 (V/V), with a flow rate of 0.8 mL min^{-1}. UV detection was performed at 213 nm, and the column temperature was 35 °C. Before HPLC analysis, the extracted samples were centrifuged at 4000 rpm for 15 min and the supernatant liquids were filtered using a PTFE syringe filter, 33 mm × 0.22 **1**m.

3. Results and discussion

3.1. Characterisation of CoO/rGO

The morphological structure of the resulting CoO/rGO was investigated by SEM and is shown in Fig. 1a. As shown in the SEM image, many CoO nanoparticles with sphere-like morphology are homogeneously anchored on the surface of the rGO sheets. The EDS elemental mapping analysis suggests the presence of Co, C, and O components in the hybrid (Fig. 1b). The atomic ratio of Co to O is 1:1, which is in complete accordance with the stoichiometry of CoO. Si signal aroused from the Si substrate. The corresponding particle size distribution is shown in Fig. 1c, revealing sphere-like CoO nanoparticles with an average size of 39.94 ± 0.62 nm.

XRD was used to investigate the phase structure of the resulting hybrids (Fig. 1d). The as-prepared GO displays a characteristic (002) peak at 9.4°, which is in good agreement with previous re- ports (Feng et al., 2013). The XRD pattern of the CoO/rGO hybrid exhibits crystalline CoO diffraction peaks, which are in good agreement with the standard CoO (JCPDS Card: 75-0533) (Li et al., 2012). This result indicates successful synthesis of CoO. A broad (002) peak was detected at approximately 24.2°, which can be indexed as disordered stacked graphitic sheets. This finding indicates that GO is reduced to rGO, which is similar to previous reports (Kim, Seo, Kim, Kim, & Kang, 2011; Wang, Huang, Tong, Li, & Chen, 2013).

Fig. 2 shows the XPS survey of the CoO/rGO. The sharp peaks in Fig. 2a correspond to the characteristic peaks of C1s, O1s, and Co2p, indicating the existence of carbon, oxygen, and cobalt elements in the sample, respectively. The Co2p XPS spectrum is given in Fig. 2b, where the binding energies are at 780.4 eV for Co2p3/2 and 796.2 eV for Co2p1/2, with the corresponding satellite structures at 786.7 and 802.5 eV can be ascribed to CoO species (Shi et al., 2012). The C1s XPS spectrum of GO (Fig. 2c) can be deconvoluted into four peaks arising from CAC/C@C (284.6 eV) in the aromatic rings, CAO (286.4 eV) of epoxy and alkoxy, C@O (287.8 eV), and OAC@O (289.3 eV) groups. For CoO/rGO (Fig. 2d), the intensity of the oxygenated groups significantly decreased, indicating that GO was reduced to rGO through the synthesis procedure (Akhavan, Choobtashani, & Ghaderi, 2012; Jung et al., 2013). This result is in a good agreement with the results of XRD.

3.2. Electrochemical behaviour of carbofuran and carbaryl at CoO/rGO/GCE

A series of nonenzymatic sensors was constructed to evaluate the electrocatalytic oxidation performance of the as-prepared CoO/rGO nanocomposite toward CBF and CBR. The effectiveness of these sensors for the oxidation of CBF and CBR was assessed by cyclic voltammetry (CV) in the selected electrolyte [0.1 M pH 4.0 Britton–Robinson buffer/acetonitrile (10:1, V/V), N_2 saturated].

As shown in Fig. 3a, CoO/rGO (curve 1) demonstrated a clear catalytic activity to CBF oxidation with a much more positive onset

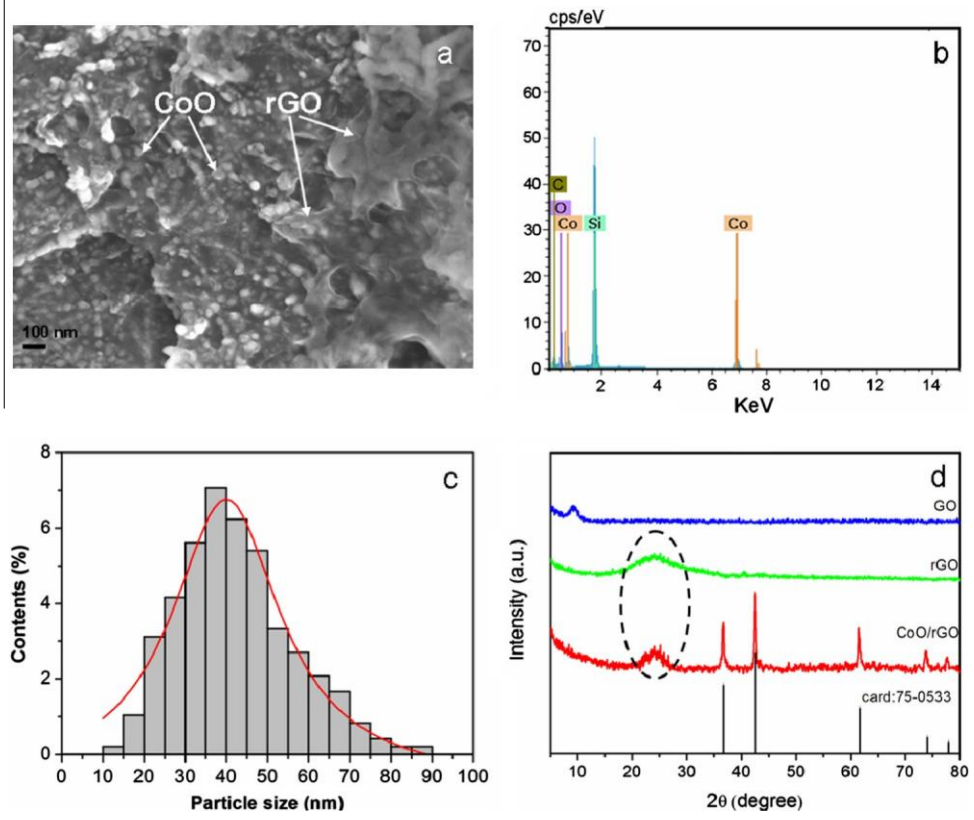

Fig. 1. (a) SEM image, (b) EDS spectrum, (c) particle size distribution histograms of the CoO/rGO and (d) XRD patters of GO, rGO and CoO/rGO.

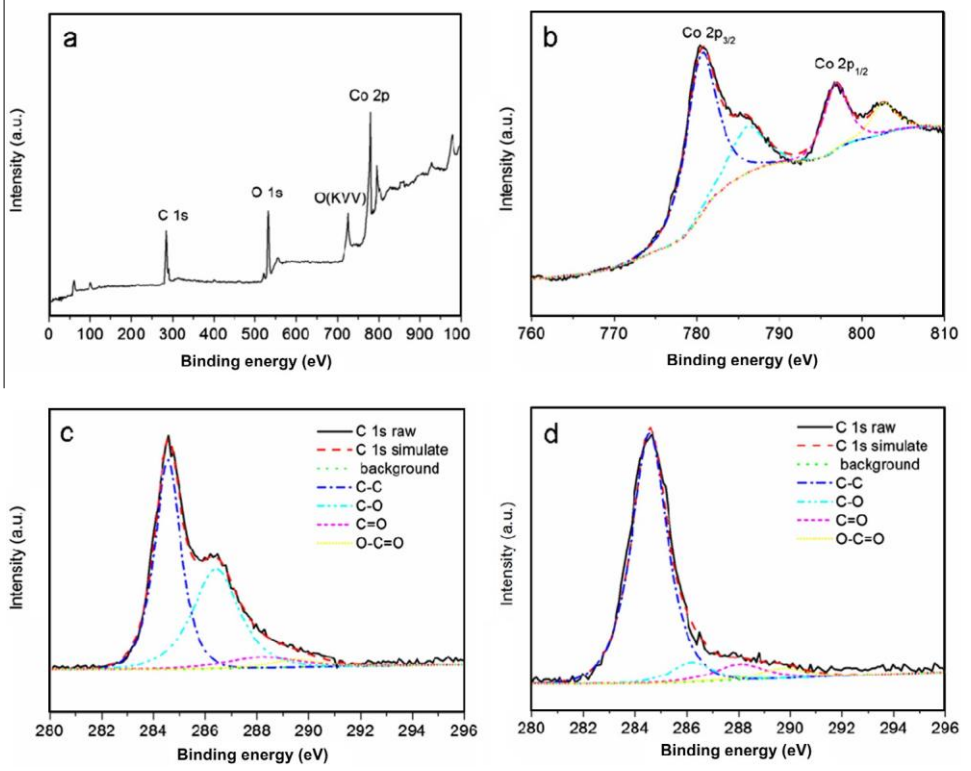

Fig. 2. (a) XPS survey spectra of CoO/rGO; (b) Co2p XPS of CoO/rGO and (c, d) C1s XPS for GO and CoO/rGO.

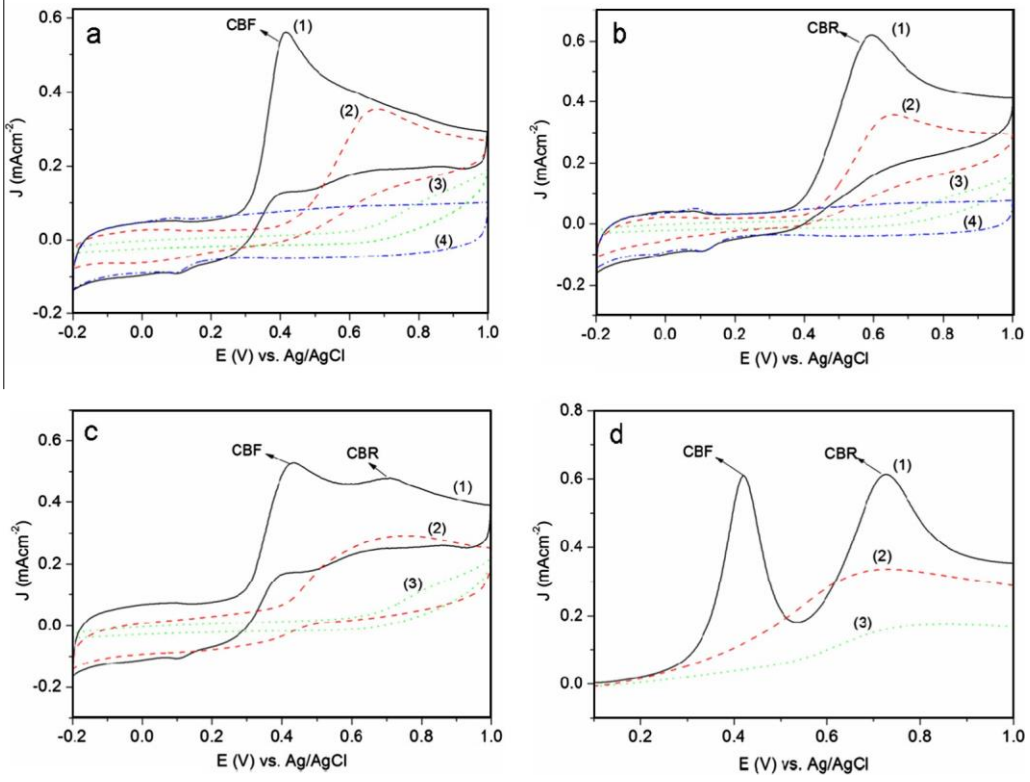

Fig. 3. CV curves of 30 **1**M CBF (a) and 70 **1**M CBR (b) on CoO/rGO (curve 1), rGO (curve 2) and CoO (curve 3) modified GCEs. (Curve 4: CV curve of CoO/rGO/GCE in the absence of CBF and CBR). (c) CV and (d) DPV curves of 30 **1**M CBF and 70 **1**M CBR in a mixture solution with CoO/rGO (curve 1), rGO (curve 2) and CoO (curve 3) modified GCEs. Electrolyte solution: 0.1 M pH 4.0 Britton–Robinson buffer/acetonitrile (10:1, V/V), N_2 saturated; Scan rate: 100 mV/s.

potential and a higher cathodic current but exhibited no electrochemical response in the absence of CBF (curve 4). By contrast, individual rGO (curve 2) and CoO (curve 3) materials exhibited very poor catalytic activity to the oxidation of CBF under identical conditions. These observations reveal that CoO/rGO exhibits notable catalytic activities and sensitivity to CBF. Electrocatalytic

oxidation of CBR was also found on the CoO/rGO-modified GCE (curve 1, Fig. 3b). The catalytic oxidation current of CBR on CoO/rGO was two times higher than that on pure rGO, whereas no obvious catalytic oxidation peak was observed on the pure CoO-modi- fied electrode under identical testing conditions. This result further confirms that the CoO/rGO nanocomposite has a superior activity for catalytic CBF and CBR oxidation. Thus, the sensitivity of the CoO/rGO sensor can be improved greatly for the determination of CBF and CBR. The lower oxidation potential also helps avoid the co-oxidation of other interferences that may coexist in fruit and vegetable samples. In addition, the CV peak of CBF oxidation appeared at 0.42 V, which is 0.29 V more negative than that of CBR oxidation. Thus, simultaneous determination of CBF and CBR can be conducted on CoO/rGO/GCE.

3.3. Electrocatalytic oxidation of CBR and CBF in a mixture

The electrochemical behaviours of CBF and CBR in a mixture were studied using CV and DPV to establish a sensitive and selective method for the quantitative determination of CBF and CBR. Fig. 3c and d shows the CV and DPV responses of CBF and CBR in a mixed solution with CoO/rGO/GCE (curve 1) as compared with rGO/GCE (curve 2) and CoO /GCE (curve 3).

The electrochemical response of CBF and CBR were resolved into two well-separated CV peaks at approximately 0.42 and 0.71 V with CoO/rGO/GCE and into one broad and overlapped anodic peak with rGO/GCE or CoO/GCE. However, better-resolved peaks were obtained by DPV, i.e., two peaks at 0.41 and 0.72 V for the oxidation of CBF and CBR, respectively (Fig. 3d). The 0.31 V peak separation between CBF and CBR was large enough to determine CBF and CBR individually and simultaneously.

3.4. Optimisation studies

3.4.1. Effect of supporting electrolytes and pH

The waves of DPV for CBF (30 **1**M) and CBR (70 **1**M) with CoO/rGO/GCE were compared in different supporting electrolytes, namely, 0.1 M Britton–Robinson buffer, 0.2 M sodium acetate–acetic acid buffer, 0.1 M phosphate buffer, carbonate buffer, and bo- rate buffer solution. The highest peak current was obtained with 0.1 M Britton–Robinson buffer/acetonitrile (10:1, V/V) as the electrolyte. Thus, 0.1 M Britton–Robinson buffer/acetonitrile (10:1, V/V) was chosen as the analytical medium, in which the peak shape was well defined. The 10:1 volumetric ratio of buffer solution to acetonitrile not only guarantees complete the dissolution of the analyst during the measurements, but also avoids the influence of acetonitrile in the electrochemical measurements.

As shown in Fig. SI-1, the effects of pH on the DPV peak current of CBF (30 **1**M) and CBR (70 **1**M) with CoO/rGO/GCE were also studied in 0.1 M Britton–Robinson buffer (pH 3.0–9.0). The maximum current appeared at pH 4.0 for the determination of both CBF and CBR. In the following experiment, pH 4.0 was selected.

3.4.2. Effect of the mass ratio of CoO to rGO in the hybrids

Further investigation of electroactivities using the various ratios of CoO to rGO was preliminarily studied to optimise the catalytic performance of CoO/rGO/GCE toward CBF and CBR. The mass ratio of CoO:rGO was varied from 1:0.25 to 1:0.5, 1:1, 1:2, and 1:4; the highest peak current was obtained at a mass ratio of 1:2. The catalytic activity of the as-prepared CoO/rGO hybrid for CBF and CBR oxidation was under the synergistic effect of the core component (CoO) and the support component (rGO). The combination of rGO with CoO is an ideal strategy of improving the catalytic performance of CoO by enhancing its charge transfer efficiency. However, excessive rGO in the composite can also decrease the loading level of CoO. Thus, the mass ratio of CoO/rGO has an important influence on the catalytic oxidation reactions of CBF and CBR. The optimum catalytic performance was achieved from CoO/rGO with a mass ratio of 1:2.

3.4.3. Effect of accumulation

The effects of accumulation potential and time on the oxidation peak current of CBF and CBR with CoO/rGO/GCE were investigated by DPV. The peak currents of CBF and CBR changed slightly as the accumulation potential changed, indicating that the accumulation potential had no influence on the peak current of CBF and CBR at CoO/rGO/GCE. Thus, an open-circuit accumulation was selected for determination of CBF and CBR. The oxidation peak current increased gradually as the accumulation time was extended from 2 to 300 s, which can be attributed to the adsorption of CBF and CBR on the electrode surface. Beyond this time frame, the oxidation peak current remained steady. This result can be attributed to the saturated adsorption of CBF and CBR on the CoO/rGO-modified electrode. Thus, 300 s was selected as the accumulation time.

3.5. Calibration, reproducibility, and selectivity

Fig. 4a shows the DPV recordings at various CBF concentrations with a constant CBR concentration of 70 **1**M under the optimised conditions for CoO/rGO/GCE. The peak currents of CBF increased with increasing concentration of CBF in the presence of CBR. The DPV curves clearly indicate that 70 **1**M CBR has no interference with the determination of CBF within the concentration range of 0.2–70 **1**M. Similarly, the oxidation peak currents of CBR increased with its increasing concentration from 0.5 to 200 **1**M when the concentration of CBF (30 **1**M) was kept constant (Fig. 4c) in a CBF and CBR mixed solution. The corresponding regression equation can be expressed as J_{CBF} (mA/cm^{-2}) = 0.24877 + 0.07045C (**1**M) (R = 0.9996) for CBF and as J_{CBR} (mA/cm^{-2}) = 1.39453 + 0.01952C (**1**M) (R = 0.9995) for CBR. The detection limit was calculated as 4.2 **1**g/L for CBF and 7.5 **1**g/L for CBR (S/N = 3).

Successive measurements using CoO/rGO/GCE were examined in a CBF and CBR mixed solution. Electrode fouling was observed after several scans. The oxidation peak currents of CBF and CBR deceased gradually because of the adsorption of the oxidation prod- ucts of CBF and CBR. However, the CoO/rGO/GCE system can be perfectly cleaned by scanning in saturated Na_2CO_3 solution from −1.0 to 1.4 V for 10 cycles, as demonstrated by a previous study (Wei et al., 2008). The catalytic activity of CoO/rGO/GCE was regained after electrochemical treatment. A relative standard deviation (RSD) of 2.9% was obtained for five successive measurements of CBF (30 **1**M) and CBR (70 **1**M). The electrode-to-electrode reproducibility (RSD, n = 5) for CBF (30 **1**M) and CBR (70 **1**M) with freshly prepared modified electrode was determined as 3.8%. The long-term storage stability of CoO/rGO/GCE was investigated under the storage conditions (exposure to air and ambient temperature). The current responses decreased only by 3.2% over the first 7 days and 8.3% for the following month, as determined by daily measurements of CBF and CBR.

The comparison of the performance of this sensor with other nonenzymatic sensors for CBF or CBR detection is listed in Table 1. As shown in the table, the detection limit and linear calibration range of the new sensor are comparable with and even better than those obtained by other hybrid-modified electrodes.

3.6. Interferences

The oxidation peak currents of CBF and CBR in the absence and presence of foreign species were measured by DPV under the above optimised conditions. The following foreign species did not interfere with the oxidation signal of CBF and CBR (i.e., signal change below 10%): 100-fold of Na^+, K^+, Mg^{2+}, Ca^{2+}, Zn^{2+}, Al^{3+}, F^-, Cl^-,

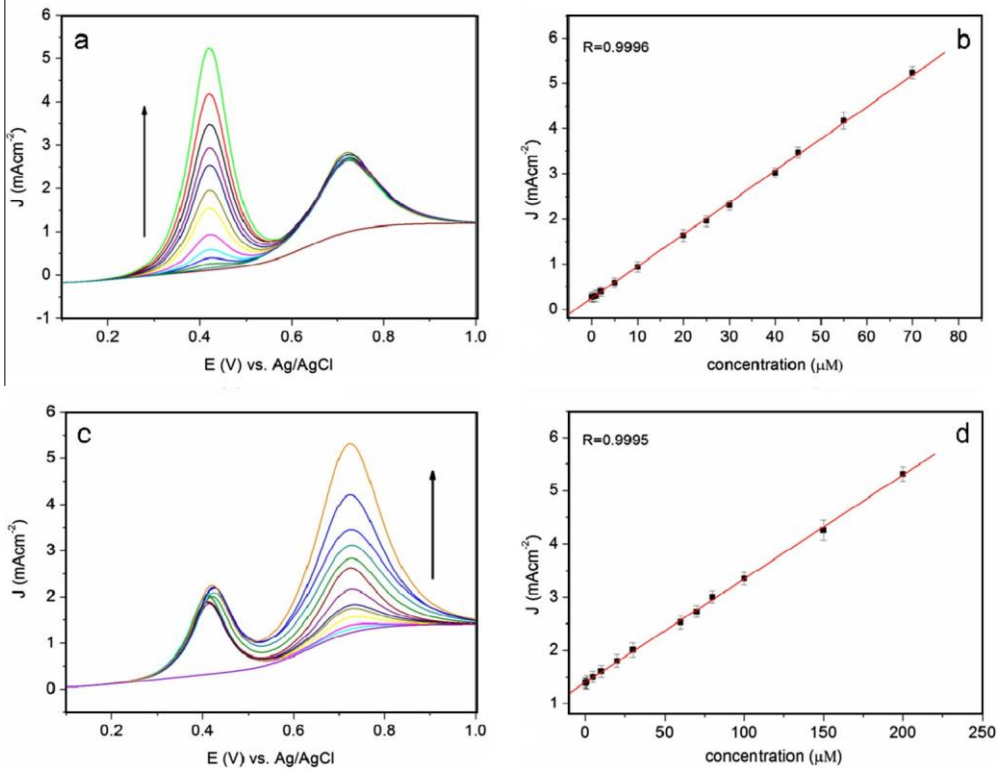

Fig. 4. (a) DPV curves of CBF oxidation with various concentration 0, 0.2, 1, 2, 5, 10, 20, 25, 30, 40, 45, 55, 70 1M (from inner to outer) in the presence of 70 1M CBR at CoO/rGO/GCE. (b) Plots of electrocatalytic peak currents from (a) versus CBF concentrations. (c) DPV curves of CBR oxidation with various concentration 0, 0.5, 1, 5, 10, 20, 30, 60, 70, 80, 100, 150, 200 1M (from inner to outer) in the presence of 30 1M CBF at CoO/rGO/GCE and (d) plots of electrocatalytic peak currents from (c) vs. CBR concentrations.

Table 1
Comparison of analytical characteristics of non-enzymatic sensors for the detection of CBF and CBR.

Configuration of sensor	Analyst	Detection limit (1g/L)	Linear range (1M)	Reference
MWCNT/CoPC/GCE	CBR	1.09	0.33–6.61	Moraes et al. (2009)
Boron-doped diamond electrode	CBR	8.2	2.5–30	Garbellini et al. (2009)
Heated screen-printed carbon electrode	CBF	10	0.4–400	Wei et al. (2008)
CoO/rGO/GCE	CBR	7.5	0.5–200	This work
	CBF	4.2	0.2–70	This work

Table 2
Simultaneous determination of CBF and CBR in fruit and vegetable samples.

Samples	Analyst	Added (1M)	By this method[a] (1M)	By HPLC[a] (1M)	Rel error (%)	Recovery (%)	RSD (%)
Grapes	CBF	0.50	0.52	0.51	1.96	104.0	2.2
	CBR	5.00	5.13	5.19	−1.16	102.6	4.7
Oranges	CBF	1.00	1.03	1.07	−3.74	103.0	3.7
	CBR	10.00	9.66	9.59	0.73	96.6	3.5
Tomato	CBF	0.50	0.48	0.51	−5.88	96.0	3.8
	CBR	5.00	4.86	4.82	0.83	97.2	2.5
Cabbages	CBF	1.00	1.02	1.03	−0.97	102.0	3.3
	CBR	10.00	10.21	10.09	1.19	102.1	4.1

[a] Each value is the average of three determination.

CO_3^{2-}; SO_4^{2-}; and NO_3^-; 10-fold of hydroquinone, xanthine, and guanine; and 8-fold of phenol, catechol, and caffeine. Inorganic ions cannot be deposited on the electrode surface, thus explaining the observed absence of significant interference. However, some phenols exerted some influence on the oxidation signal.

Interferences arising from other carbamate pesticide were also used to evaluate the selectivity of CoO/rGO sensor to CBF and CBR. Isoprocarb, methiocarb and propoxur were chosen for the selectivity test. Separate DPV experiments were performed with CBF (30 1M) and CBR (70 1M) in 0.1 M electrolyte solution in the presence of 100 1M isoprocarb, methiocarb or propoxur (see Supporting information SI-2). The results showed that the oxidation of these three compounds occurred at different potentials. The oxidation peak of isoprocarb, methiocarb and propoxur were at 0.18, 0.25 and 0.20 V, respectively, while they are at 0.42 and 0.71 V for CBF and CBR. One can see that these three carbamate pesticides do not interfere with the detection of CBF and CBR, since the oxidation peak potential separation was large. Meanwhile, the results

showed that the peak heights from CBF (30 **1**M) and CBR (70 **1**M) were higher than those for 100 **1**M isoprocarb, methiocarb and propoxur by almost 10 times. Thus, this CoO/rGO sensor provided and excellent selectivity for CBF and CBR.

3.7. Analysis of real samples

CoO/rGO/GCE was used to detect CBF and CBR in some fruit and vegetable samples to evaluate the practical application of this sensor. As shown in Table 2, all samples were either contaminated with concentrations below the detection limit or absolutely free of CBF and CBR. A recovery study was carried out with the sensors using the standard addition method and direct interpolation in the linear regression. The determined values were in agreement with the assigned value for each substrate in the samples. The satisfactory recoveries (96.0–104.0%) of CoO/rGO/GCE for CBF and CBR detection in fruit and vegetable samples confirm that this material is a stable and sensitive sensor for analysing real samples. The concentration of CBF and CBR were also analysed by HPLC. The analysis of statistically significant difference of the two techniques showed that the results obtained with this sensor were in satisfactory agreement with data from the reference method obtained at 95% confidence level using the paired *t*-test model. This finding indicates that this sensor has good accuracy for CBF and CBR detection in real samples.

4. Conclusions

Heterogeneous CoO/rGO was synthesized and developed to fabricate a novel nonenzymatic sensor. The as-synthesized CoO/rGO sensor displayed an excellent electrocatalytic activity toward CBF and CBR oxidation, and was successfully applied for the simultaneous detection of CBF and CBR in fruit and vegetable samples. The simple fabrication procedure, wide linear range, low detection limit, and high stability present this sensor as an attractive candidate for practical application.

Acknowledgements

This work was supported by National Natural Science Foundation of China (Grant Nos. 51202079 and 21201070). A project funded by the Priority Academic Program development of Jiangsu Higher Education Institutions. The authors are grateful to National College Student's Innovation Project and the young teachers of Jiangsu Province universities' "blue and green blue project". The authors also acknowledge the Australian National Fabrication Facility (ANFF) for provision of services and equipment access.

References

Akhavan, O., Choobtashani, M., & Ghaderi, E. (2012). Protein degradation and RNA efflux of viruses photocatalyzed by graphene–tungsten oxide composite under visible light irradiation. *The Journal of Physical Chemistry C, 116*, 9653–9659.

Akinbulu, I. A., Khene, S., & Nyokong, T. (2010). Surface properties of self-assembled monolayer films of tetra-substituted cobalt, iron and manganese alkylthio phthalocyanine complexes. *Electrochimica Acta, 55*, 7085–7093.

Akinbulu, I. A., Ozoemena, K. I., & Nyokong, T. (2011). Formation, surface characterization, and electrocatalytic application of self-assembled monolayer films of tetra-substituted manganese, iron, and cobalt benzylthio phthalocyanine complexes. *Journal of Solid State Electrochemistry, 15*, 2239–2251.

Cavaliere, B., Monteleone, M., Naccarato, A., Sindona, G., & Tagarelli, A. (2012). A solid-phase microextraction-gas chromatographic approach combined with triple quadrupole mass spectrometry for the assay of carbamate pesticides in water samples. *Journal of Chromatography A, 1257*, 149–157.

Cesarino, I., Moraes, F. C., Lanza, M. R. V., & Machado, S. A. S. (2012). Electrochemical detection of carbamate pesticides in fruit and vegetables with a biosensor based on acetylcholinesterase immobilized on a composite of polyaniline–carbon nanotubes. *Food Chemistry, 135*, 873–879.

Codognoto, L., Tanimoto, S. T., Pedrosa, V. A., Suffredini, H. B., Machado, S. A. S., & Avaca, L. A. (2006). Electroanalytical determination of carbaryl in natural waters on boron doped diamond electrode. *Electroanalysis, 18*, 253–258.

Du, D., Wang, M., Cai, J., Tao, Y., Tu, H., & Zhang, A. (2008). Immobilization of acetylcholinesterase based on the controllable adsorption of carbon nanotubes onto an alkanethiol monolayer for carbaryl sensing. *Analyst, 133*, 1790–1795.

Feng, Z., Zhang, C., Chen, J., Wang, Y., Jin, X., Zhang, R., et al. (2013). An easy and eco-friendly method to prepare reduced graphene oxide with $Fe(OH)_2$ for use as a conductive additive for $LiFePO_4$ cathode materials. *RSC Advances, 3*, 4408–4415.

Firdoz, S., Ma, F., Yue, X., Dai, Z., Kumar, A., & Jiang, B. (2010). A novel amperometric biosensor based on single walled carbon nanotubes with acetylcholine esterase for the detection of carbaryl pesticide in water. *Talanta, 83*, 269–273.

Garbellini, G. S., Salazar-Banda, G. R., & Avaca, L. A. (2009). Sonovoltammetric determination of toxic compounds in vegetables and fruits using diamond electrodes. *Food Chemistry, 116*, 1029–1035.

Hummers, W. S., & Offeman, R. E. (1958). Preparation of graphitic oxide. *Journal of the American Chemical Society, 80*. 1339-1339.

Jung, H. G., Jeong, Y. S., Park, J. B., Sun, Y. K., Scrosati, B., & Lee, Y. J. (2013). Ruthenium-based electrocatalysts supported on reduced graphene oxide for lithium–air batteries. *ACS Nano, 7*, 3532–3539.

Kim, H., Seo, D. H., Kim, S. W., Kim, J., & Kang, K. (2011). Highly reversible Co_3O_4/graphene hybrid anode for lithium rechargeable batteries. *Carbon, 49*, 326–332.

Li, M., Yin, Y. X., Li, C., Zhang, F., Wan, L. J., Xu, S., et al. (2012). Well-dispersed bi-component-active $CoO/CoFe_2O_4$ nanocomposites with tunable performances as anode materials for lithium-ion batteries. *Chemical Communications, 48*, 410–412.

Liu, T., Su, H., Qu, X., Ju, P., Cui, L., & Ai, S. (2011). Acetylcholinesterase biosensor based on 3-carboxyphenylboronic acid/reduced graphene oxide–gold nanocomposites modified electrode for amperometric detection of organophosphorus and carbamate pesticides. *Sensors and Actuators B: Chemical, 160*, 1255–1261.

March, C., Manclus, J. J., Jimenez, Y., Arnau, A., & Montoya, A. (2009). A piezoelectric immunosensor for determination of pesticide residues and metabolites in fruits juices. *Talanta, 78*, 827–833.

Moraes, F. C., Mascaro, L. H., Machado, S. A. S., & Brett, C. M. A. (2009). Direct electrochemical determination of carbaryl using a multi-walled carbon nanotube/cobalt phthalocyanine modified electrode. *Talanta, 79*, 1406–1411.

Nikolelis, D. P., Raftopoulou, G., Psaroudakis, N., & Nikoleli, G. P. (2008). Development of an electrochemical biosensor for the rapid detection of carbofuran based on air stable lipid films with incorporated calix[4]arene phosphoryl receptor. *Electroanalysis, 20*, 1574–1580.

Oliveira, T. M. B. F., Barroso, M. F., Morais, S., Araujo, M., Freire, C., Lima-Neto, P. D., et al. (2013). Laccase–Prussian blue film–graphene doped carbon paste modified electrode for carbamate pesticides quantification. *Biosensors and Bioelectronics, 47*, 292–299.

Rao, T. N., Loo, B. H., Sarada, B. V., Terashima, C., & Fujishima, A. (2002). Electrochemical detection of carbamate pesticides at conductive diamond electrode. *Analytical Chemistry, 74*, 1578–1583.

Sanchez-Barragan, I., Karim, K., Costa-Fernadez, J. M., Piletsky, S. A., & Sanz-Medel, A. (2007). A molecularly imprinted polymer for carbaryl determination in water. *Sensors and Actuators B: Chemical, 123*, 798–804.

Shi, R., Chen, G., Ma, W., Zhang, D., Qiu, G., & Liu, X. (2012). Shape-controlled synthesis and characterization of cobalt oxides hollow spheres and octahedra. *Dalton Transactions, 41*, 5981–5987.

Song, X. Y., Shi, Y. P., & Chen, J. (2013). Carbon nanotubes-reinforced hollow fibre solid-phase microextraction coupled with high performance liquid chromatography for the determination of carbamate pesticides in apples. *Food Chemistry, 139*, 246–252.

Sun, X., Du, S., & Wang, X. (2012). Amerometric immunosensor for carbofuran detection based on gold nanoparticles and PB-MWCNTs-CTS composite film. *European Food Research and Technology, 235*, 469–477.

Veglia, A. V. (2000). Fluorimetric determination of carbamate pesticides in host–guest complexes. *Molecules, 5*, 437–438.

Wang, M. Y., Huang, H. R., Tong, Z. W., Li, W. H., & Chen, J. (2013). Reduced graphene oxide–cuprous oxide composite via facial deposition for photocatalytic dye-degradation. *Journal of Alloys and Compounds, 568*, 26–35.

Wei, H., Sun, J. J., Wang, Y. M., Li, X., & Chen, G. N. (2008). Rapid hydrolysis and electrochemical detection of trace carbofuran at a disposable heated screen- printed carbon electrode. *The Analyst, 133*, 1619–1624.

Zhang, L., Long, L., Zhang, W., Du, D., & Lin, Y. (2012). Study of inhibition, reaction and aging process of pesticides using graphene nanosheets/gold nanoparticles-based acetylcholinesterase biosensor. *Electroanalysis, 24*, 1745–1750.